

A new ripplon branch in He II

I.V. Tanatarov*

*National Science Center "Kharkov Institute of Physics and Technology",
Academicheskaya St. 1, Kharkov, 61108, Ukraine*

I.N. Adamenko and K.E. Nemchenko

Karazin Kharkov National University, Svobody Sq. 4, Kharkov, 61077, Ukraine

A.F.G. Wyatt

School of Physics, University of Exeter, Exeter EX4 4QL, UK

(Dated: June 9, 2011)

We analyse the dispersion relation of ripplons, on the surface of superfluid helium, using the dispersive hydrodynamics approach and find a new ripplon branch. We obtain analytical equation for the dispersion relation and analytic expressions for the limiting cases. We discuss where ripplons can exist in the energy-wavenumber plane. A numerical solution for the ripplon dispersion curve is obtained in the allowed regions. The new ripplon branch is found at energies just below the instability point.

I. INTRODUCTION

Ripplons are quantised capillary waves on the free surface of superfluid ^4He . At low frequencies the dispersion law gives a good way of measuring the surface tension of liquid helium [1, 2]. The temperature dependence of the surface tension is due to ripplons [3]. Ripplons can be detected by neutron scattering, in a similar way to the bulk modes, and have been shown to exist up to wavenumber of 1.5 \AA^{-1} , where the ripplon energy is equal to that of the roton minimum, 8.6 K, [4, 5]. Ripplons are the dominant scatterer of surface state electrons on liquid helium (see [6, 7] and references therein). Ripplons play a significant role in the condensation [8], evaporation and reflection of atoms from liquid ^4He , [9, 10]. It has been suggested that ripplons are the most favourable excitations for the simulation of general-relativistic effects related to horizons of white holes [11].

Ripplons are well defined excitations and so have a reasonably long lifetime, but they can be scattered by phonons and rotons, and by other ripplons. At low energies there can be three ripplon scattering, in an analogous process to three phonon scattering. However for low energy ripplons at low temperatures, the ripplon lifetime is dominated to phonon scattering rather than ripplon-riplon scattering [12].

In this paper we present a theoretical model of ripplons which is good enough to account for the measured dispersion curve $\omega(k)$ but is simple enough to expose the underlying physics. It explains why ripplons only exist in certain parts of the (ω, k) plane, and why the dispersion curve approaches the line $\omega = \Delta_{rot}$ at the top of a parabola, where Δ_{rot} is the energy of the roton minimum. Moreover the model predicts a new roton branch at energies $< \sim 2\Delta_{rot}$.

The theoretical model is a non-local hydrodynamical theory [13], developed by us in Ref. [14]. The actual physical characteristics of the liquid are introduced into the model by using the measured dispersion curve for bulk excitations. The justification of application of non-local hydrodynamics to the description of a quantum fluid at interatomic distances is given in [14], and in more detail in [15]. It is based on the fact, that in a quantum fluid the atoms are delocalized, as their thermal de Broglie wavelength is greater than the atom spacing. The general idea of description of a quantum fluid in terms of hydrodynamic variables at interatomic scales is being widely used. One of the first to exploit it was Atkins in 1959 [16], when he introduced bubbles and snowballs of microscopic size in order to describe the mobility of electrons and ions in He II by means of methods of theory of continuous medium. The idea is utilized now in the variations of density functional theory (see for example [17]), and is implicitly assumed in other fields of research related to superfluidity. In particular, the variables of continuous media are used lately for description of vortices in helium with dimensions of the order of the interatomic distances [18].

The quantum fluid, which is considered continuous at any length scales, can be described in terms of the variables of continuous media, which satisfy the mass and momentum conservation laws. The equations of ideal liquid, which follow from them, do not form a closed system, and are supplemented by the equation of state, which specifies the functional relation between pressure and density. As shown in [14, 15], the equation of state for small deviations of the system from equilibrium in the general case is non-local, with some difference kernel $h(\mathbf{r})$.

The closed linear system of equations is brought to a non-local integro-differential wave equation with regard to pressure. The dispersion relation of the fluid $\Omega(k)$ then is determined by the Fourier transform of the kernel $h(\mathbf{r})$ and can contain arbitrary degrees of k . In this paper we

* igor.tanatarov@gmail.com

start from the dispersion relation that approximates the experimental data for the spectrum of superfluid helium. The chosen $\Omega(k)$ gives explicit expression for the kernel $h(\mathbf{r})$, which determines the equation of state and the non-local wave equation.

In order to derive the dispersion relation of ripplons, we look for the solution of the nonlocal wave equation (1) in half-space, equipped with usual boundary conditions (2). The use of simple model of superfluid helium allows us to fully solve the problem of ripplons' spectrum. The ripplons' dispersion equation is obtained in algebraic form, and its analytic solutions are derived in limiting cases. The analytic and numerical results of the paper in the region below the roton gap are consistent with the experiments, numerical computations and qualitative estimates of other authors [4],[17].

A preliminary and partial account of this analysis is given in [19], where a very approximate function for the dispersion curve for bulk phonons and rotons was used. This was useful to show that the method had promise but it could not show the new ripplon branch or other features. Here we use a much more detailed function for the phonon-roton dispersion $\Omega(k)$, which gives an excellent approximation of the experimentally measured curve over the whole wave vector range. This allows us to describe the ripplons in detail in the whole energy interval. This range includes the energy of the Pitaevskii instability at twice the roton minimum energy [20]. It is just below this energy where we find a new ripplon branch.

II. EQUATIONS AND BOUNDARY CONDITIONS

Let us consider the half-space $z > 0$ filled by superfluid helium. Following the approach in Ref. [14], the liquid obeys the ordinary linearized equations of an ideal liquid, but the relation between the deviations P and ρ of pressure and density from the respective equilibrium values is nonlocal, with some difference kernel $h(\mathbf{r})$ [14, 15].

$$\Delta P(\mathbf{r}, t) = \int_{z_1 > 0} d^3 r_1 h(|\mathbf{r} - \mathbf{r}_1|) \ddot{P}(\mathbf{r}_1, t), \quad z \in (0, \infty). \quad (1)$$

Here the dots denote derivatives by time.

We assume that the interface is sharp enough so that the kernel $h(r)$ is the same near the interface as it is in the bulk medium. The kernel is related to the dispersion relation of the bulk excitations $\Omega(k)$ through its Fourier transform (see [14]) $h(k) = k^2 / \Omega^2(k)$.

The dispersion relation $\Omega(k)$, is for the continuous medium which fills the half-space $z > 0$. It is nonlinear and has the distinctive form of the dispersion of phonons and rotons in superfluid helium (see Fig.1), and the characteristic length of the kernel is of the order of average interatomic separation.

The equation (1) is supplemented by the boundary condition at the free surface. The pressure at the surface

with surface tension σ , must include the Laplace term, which for small deviations of the surface from equilibrium is

$$P = \sigma \left(\frac{\partial^2 \xi}{\partial x^2} + \frac{\partial^2 \xi}{\partial y^2} \right), \quad (2)$$

where ξ is the z -coordinate of the points of the surface (see for example [13] or [21]).

All the variables have the form $\sim \exp(i\mathbf{k}\mathbf{r} - i\omega t)$. For a given frequency ω and the projection of wave vector \mathbf{k} on the plane of the free surface (x, y) , \mathbf{k}_τ , this expression becomes $P = -\sigma k_\tau^2 \xi$. The z -component of velocity of the surface is $v_z = -i\omega \xi$. We can therefore write the boundary condition in the form

$$v_z|_{z=0} = \frac{i\omega}{\sigma k_\tau^2} P|_{z=0}. \quad (3)$$

III. EQUATION FOR THE DISPERSION RELATION OF RIPPLONS AND ANALYTICAL SOLUTIONS

The dispersion relation, for undamped waves, can in general be written $\omega^2 = \Omega^2(k^2)$. We express the function $\Omega^2(k^2)$ as a polynomial of degree S in powers of k^2 , such that the only real zero of $\Omega^2(k^2)$ is at $k^2 = 0$. Near this point $\Omega^2 \sim k^2$. After some analysis, the Fourier image by \mathbf{r} and t of the solution of equation (1) can be written in the form (see [15] and references cited there):

$$P(k_z; \mathbf{k}_\tau, \omega) = \frac{C_{out}(\omega, \mathbf{k}_\tau)}{k_z - k_{1z}(\omega, \mathbf{k}_\tau)} \prod_{k_{iz} \in \mathcal{C}_+} \frac{k_z - k_{iz}(0, \mathbf{k}_\tau)}{k_z - k_{iz}(\omega, \mathbf{k}_\tau)}. \quad (4)$$

Here $\mathbf{k} = \mathbf{k}_\tau + \mathbf{e}_z k_z$ is the wave vector. The product is taken over all the roots $k_z = k_{iz}$ of equation $\Omega^2(k^2 = k_\tau^2 + k_z^2) = \omega^2$ in the upper half-plane \mathcal{C}_+ of the complex variable k_z . The real roots are assumed to be shifted up from the real axis. The root $k_{1z}(\omega, \mathbf{k}_\tau)$ is the phonon root, i.e. the one in \mathcal{C}_+ , which continuously goes to zero at $\omega = 0$ and $k_\tau = 0$. The prime superscript on the product designates that k_{1z} is excluded from the product. The function $C_{out}(\omega, \mathbf{k}_\tau)$ is the amplitude of the wave.

Ripplons have solutions which are damped with distance from the liquid's surface. These occur for all the k_{iz} , that are not real. For a given value of ω , the imaginary k_{iz} occur when k_τ^2 is greater than any of the real roots $k_i^2(\omega)$ of equation $\Omega^2(k^2) = \omega^2$.

The dispersion relation for superfluid helium is shown in Fig.1. We assign subscripts to the positive roots of equation $\Omega^2(k^2) = \omega^2$ in the ascending order of their absolute values, i.e. k_1 , k_2 and k_3 are phonons, R^- and R^+ rotons respectively.

The inverse Fourier transform of (4) is calculated from the residues in \mathcal{C}_+ , and velocity is obtained from the relation $\partial \mathbf{v} / \partial t = -\nabla P / \rho_0$ where ρ_0 is the equilibrium density. Then the values of P and v_z , on the surface $z = 0$, can be expressed in terms of the residues of $P(k_z)$ and

$k_z P(k_z)$ at infinity. These are found directly by expanding P from (4). Then we obtain

$$v_z|_{z=0} = \frac{1}{\rho_0 \omega} \left\{ k_{1z} + \sum_{i=2}^S [k_{iz} - k_{iz}(\omega=0)] \right\} P|_{z=0}. \quad (5)$$

Comparing (5) with the boundary condition (3), we finally obtain the equation for the dispersion relation $\omega(k_\tau)$ of ripples:

$$\omega^2 = \frac{\sigma}{\rho_0} \cdot \frac{k_\tau^2}{i} \left\{ k_{1z}(\omega, k_\tau) + \sum_{i=2}^S [k_{iz}(\omega, k_\tau) - k_{iz}(0, k_\tau)] \right\}. \quad (6)$$

This equation is written in terms of $k_{iz}(\omega, k_\tau) = \sqrt{k_i^2(\omega) - k_\tau^2} \in \mathcal{C}_+$, where $k_i^2(\omega)$ in turn are the roots of the polynomial equation $\Omega^2(k^2) = \omega^2$ with real coefficients. Then taking into account the condition that all the k_{iz} are non-real, we can show, that the right part of the equation (6) is in fact real. Indeed, let us consider the equation $\Omega^2(k^2 = k_z^2 + k_\tau^2) = \omega^2$ with regard to k_z^2 . This equation is also a polynomial equation with real coefficients. So its roots with regard to k_z^2 are either negative (no positive roots exist or there would be real k_{iz}) or break up into complex-conjugate pairs. The negative roots give imaginary k_{iz} and complex-conjugate pairs k_{iz}^2, k_{jz}^2 give pairs k_{iz}, k_{jz} in \mathcal{C}_+ , such that $k_{iz} = -k_{jz}^*$, and for such a pair $k_{iz} + k_{jz} = 2i \text{Im } k_{iz}$. Therefore the expression inside of the braces in (6) is imaginary and the right hand part is real.

Further insight is obtained if we search in Eq. (6) for ω^2 in the form of a series expansion in k_τ . On substituting the expansions of all quantities by small k_τ and ω into the equation (6), we obtain within $O(k_\tau^4)$

$$\omega^2 = \frac{\sigma}{\rho_0} k_\tau^3 \left\{ 1 - \frac{\sigma k_\tau}{2\rho_0 s^2} + \frac{\sigma^2 k_\tau^2}{8\rho_0^2 s^4} + \frac{\sigma\beta}{\rho_0} \left(k_\tau^2 - \frac{\sigma}{\rho_0 s^2} k_\tau^3 \right) \right\}, \quad (7)$$

where $\beta = \frac{1}{2i} \sum_{i=2}^S k_{iz}^{-1}(0, 0) \frac{dk_{iz}^2(\omega)}{d\omega^2} \Big|_{\omega=0}$.

In the limit of small k_τ and ω , we replace the braces in Eq. (7) by unity, and so obtain the well-known dispersion of capillary waves. The second and third terms in the braces, take into account compressibility. The fourth term, proportional to β , expresses the influence of the $(S-1)$ roots k_i with $i > 1$, which include the rotons. The latter give only small correction at small ω , but with increasing frequency they become of the order of the phonon terms and, as it will be shown below, they determine the asymptotic behavior of the curve $\omega(k_\tau)$ in the proximity of $\omega = \Delta_{rot}$.

Of particular interest is the behaviour of the dispersion curve close to the roton gap $\omega = \Delta_{rot}$. In this region the functions $k_{2,3z}(\omega, k_\tau)$ contain terms $\sim \sqrt{\Delta_{rot} - \omega}$, which leads to the same square-root singularity in the equation (6): $(k_{2z} + k_{3z}) \sim \sqrt{\Delta_{rot} - \omega}$. Therefore it can be shown that the asymptote of $\omega(k_\tau)$ at $\omega = \Delta_{rot} - 0$ has the form

$$k_c - k_\tau = \frac{b}{a + c} \sqrt{\Delta_{rot} - \omega}, \quad (8)$$

where

$$a = 2 \frac{\sigma}{\rho_0} \frac{\Delta_{rot}^2}{k_c^4}; \quad b = 2 \frac{k_{rot}}{k_c} \sqrt{2 \frac{\mu}{\hbar} / (k_{rot}^2 - k_c^2)};$$

$$-ic = k_{1z}^{-1}(\Delta_{rot}, k_c) + \sum_{i=4}^S k_{iz}^{-1}(\Delta_{rot}, k_c) - \sum_{i=2}^S k_{iz}^{-1}(0, k_c);$$

k_{rot} is the momentum of a roton with energy Δ_{rot} , μ is the ‘‘roton mass’’ and k_c is determined by the condition $\omega(k_\tau = k_c) = \Delta_{rot}$. The numerical solution below, shows that this point indeed exists, is unique and $k_c < k_{rot}$, so a, b, c are all real. We see that the curve $\omega(k_\tau)$ approaches the value $\omega = \Delta_{rot}$ at the top of a parabola, and ends in the adhesion point, with zero derivative. There is no dispersion curve below Δ_{rot} with $k_\tau > k_c$. In the theory of Ref. [17] the asymptote was obtained qualitatively as one of the possible variants, from general quantum-mechanical considerations.

In Fig.1 we show the dispersion curve for bulk excitations. The areas bounded by the dispersion curve and the lines at constant energy at Δ_{rot} , Δ_{max} , and $2\Delta_{rot}$ are labelled A to G. We consider the helium surface to have a sinusoidal perturbation with wavenumber k_τ and then see if a stable ripplon solution is possible in each of the areas. A ripplon solution requires k_{1z} to be imaginary. In region A, $k_\tau < k_1$ and $k_{1z}^2 = k_1^2 - k_\tau^2$ so k_{1z} is real, and for k_{1z} real, Eq. (6) gives k_τ complex which means the ripplon decays, so no ripplon can occur in this area. The imposed perturbation would decay into phonons. In region B, k_{1z} is not real and therefore Eq. (6) gives k_τ real, so ripples can exist. They will lie on a ripplon dispersion curve in this area. In region C, k_{1z} , k_{2z} and k_{3z} are real and the perturbation decays into phonons, R^- rotons and R^+ rotons. In region D, k_{2z} and k_{3z} are real and the perturbation decays into R^- rotons and R^+ rotons. In region E, k_{3z} is real and the perturbation decays into R^+ rotons. So there are no ripples in these regions. In region F there are no solutions to Eq. (6) because of the high gradient of the dispersion curve, so there are no ripples. In region G, the gradient is smaller and there are solutions to Eq. (6) so we predict that there are ripples in this area.

IV. NUMERICAL SOLUTION AND THE NEW RIPPLON BRANCH

We find the ripplon dispersion curve numerically in the range of $k_\tau \in (0, 3) \text{ \AA}^{-1}$. It is shown on Fig.1. We see that, as predicted, the computed curve at small wave vectors is close to the classical $k_\tau^{3/2}$ law, but deviates from it at larger k_τ and approaches the level of Δ_{rot} at the top of an inverted parabola at $k_c = 1.27 \text{ \AA}^{-1}$.

There is no ripplon solution in the region to the right (see Fig.1) of the R^+ roton dispersion curve for $\omega \in (\Delta_{rot}, \Delta_{max})$. However, if we further increase ω while moving along the curve $k_3(\omega)$, as we get close to the region where $\Omega(k)/k$ reaches its maximum, the curve turns down and aims to the point of instability [20] in almost

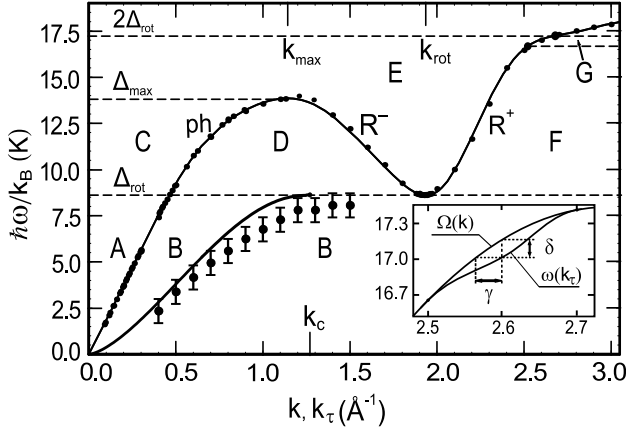


FIG. 1. The dots are experimental data for the dispersion relation of bulk excitations $\Omega(k)$ [23], and the thin line shows its analytic approximation that is used, with $S=18$. The thick line shows the results of numerical solution of Eq. (6) for the ripplon dispersion curve $\omega(k_\tau)$. Large dots with error bars are experimental data for the ripplon dispersion [4]. Two black dots in the high-energy part of the bulk spectrum designate the end points of the very high energy ripplon solution, and the insert graph shows its behaviour schematically, where $\gamma = 0.7 \cdot 10^{-3} \text{ \AA}^{-1}$ and $\delta = 1.6 \cdot 10^{-3} \text{ K}$. The different regions of the (ω, k) plane are labelled A to G. The usual ripples are in region B and the new ripples are in region G. In the other regions, ripples cannot exist, as described in the text

a straight line, the left hand part of Eq. (6) starts to change slowly. At the same time, some of the functions $k_i^2(\omega)$ for $i > 3$, which were slowly changing functions below Δ_{max} , begin to change fast and give significant contribution to right-hand part of Eq. (6), so here the ripplon solution is determined by the functions k_{iz} .

Therefore, when we search for the solutions on the R^+ roton curve, we find two common points above Δ_{max} . The first point is at 2.52 \AA^{-1} and 16.65 K , which is almost exactly at the maximum of $\Omega(k)/k$, and the second point is 2.75 \AA^{-1} and 17.30 K . The ripplon dispersion curve $\omega(k_\tau)$ between these points lies near, but below, the bulk dispersion. The two common points are adhesion points. This is partly the reason for the deviation between the curves being extremely small. At $k_\tau = 2.6 \text{ \AA}^{-1}$, midway between the two end points, the deviation is $1.6 \cdot 10^{-3} \text{ K}$ or $0.7 \cdot 10^{-3} \text{ \AA}^{-1}$, which is too small to see on the scale of the main graph, so in the inset to Fig. 1 we show this region expanded. Nevertheless the separation of the ripplon dispersion curve from the roton dispersion curve, is greatly exaggerated.

We now show that the common points of the ripplon dispersion curve $\omega(k_\tau)$ and the R^+ roton dispersion curve $k_3(\omega)$ are adhesion points. The Eq. (6) can be rewritten as $F(\omega, k_\tau) = 0$. There, the term k_{3z} in $F(\omega, k_\tau)$, goes to zero as $\sqrt{k_\tau - k_3(\omega)}$ near the R^+ roton branch. So the gradient of $F(\omega, k_\tau)$ in the plane (ω, k_τ) tends to infinity on the curve $k_\tau = k_3(\omega)$ and is directed normal to the

curve. From the other side, the gradient of $F(\omega, k_\tau)$ is directed normal to the curve $\omega(k_\tau)$, which is its level curve $F = 0$. Therefore at the common points of the two curves, the angle between them is zero, and so these points are adhesion points.

We now consider the penetration depth of the ripplon solution on this branch of the ripplon dispersion curve. At $k_\tau = 2.6 \text{ \AA}^{-1}$ the value of k_{3z} is close to its maximum 0.06 \AA^{-1} . Hence the penetration depth of the ripplon solution, determined by the term containing $\sim k_{3z}$, has a minimum value $\delta \sim |k_{3z}|^{-1} \sim 16 \text{ \AA}$, and at the end points it tends to infinity. The deviation between the two curves is second order in the small parameter k_{3z} because $|k_{3z}| \sim \sqrt{k_\tau - k_3}$.

The relatively large penetration depth of the solution means that macroscopic films or the surface of bulk helium are needed to observe these ripples. They will not be seen on films of a few monolayers. The high-energy ripples should exist and be observable on saturated films of He II, which have a typical thicknesses of 300 \AA . In the same way the penetration depth of the ripples in region B (see Fig. 1) tends to infinity when ω tends to Δ_{rot} . So the ending point of the dispersion curve (Δ_{rot}, k_c) can also be observed only in thick enough films of He II. Thus in the two most interesting regions of their dispersion curve, the ripplon solutions have large penetration depth, much larger than the characteristic distances, of several monolayers thickness, of the changes of the density profile at the free surface. The major part of the energy of the wave is stored outside of the transition layer, it can be neglected, and the surface can be considered sharp (i.e. the kernel $h(r)$ in Eq. (1) is the same as in the bulk fluid).

The numerical calculations were carried out by representing the function $\Omega^2(k^2)$ as a polynomial of degree S , with $S = 18$ and $S = 21$. The high-energy ripples solution exists in both cases, and the end points do not differ substantially. The deviation between the curves $k_3(\omega)$ and $\omega(k_\tau)$ remains very small, and is much less than the difference between the two polynomials.

We have also checked for the stability of the solution with regard to changes in surface tension σ , as at high curvatures of the surface its curvature dependence might be significant. If we decrease σ , the end points of the ripplon dispersion curve slide apart along $k_3(\omega)$. At the value $\sigma = 1.75 \text{ N/m}$ ($\sigma = 3.544 \text{ N/m}$ at zero temperature [23]), the lower adhesion point reaches the point 2.44 \AA^{-1} , 16 K . If we increase σ , then the end points slide towards each other and the solution disappears at $\sigma = 8.7 \text{ N/m}$. This shows that any realistic dependence $\sigma(k_\tau)$ can be inserted in Eq. (6) without complicating the numerical solution.

V. CONCLUSION

We have developed a non-local hydrodynamical model of ripples on the free surface of superfluid ^4He , which

uses the measured dispersion curve for phonons and rotons to include the relevant characteristics of the liquid. The model gives a very good description of the measured ripplon dispersion curve, and it accounts for the parabolic approach of the dispersion curve to the line $\omega = \Delta_{rot}$. The model gives the correct classical dispersion of capillary waves at long wavelengths. These good agreements validate the model. Furthermore the model is transparent enough to expose the physical reasons why the low energy ripplon branch lies below the phonon dispersion curve and ends at the energy Δ_{rot} . It is explained, with the aid of Fig.1, that surface perturbations, on the low k side of the phonon-roton dispersion curve, just decay to phonons or rotons and so stable ripplons can only be found on the high k side of the phonon-roton dispersion

curve. For energies $> \Delta_{max}$, and on the high k side of the phonon-roton dispersion curve, ripplon solutions of Eq.(6) are possible at energies just below $2\Delta_{rot}$. It can be shown that these ripplons are stable against decay into two ripplons with energy $< \Delta_{rot}$. That such ripplons solutions exist is unexpected and is a striking prediction of this analysis. We hope this prediction stimulates new experiments to detect these ripplons.

ACKNOWLEDGMENTS

We are grateful to EPSRC of the UK (grant EP/F019157/1) for support of this work.

-
- [1] P. J. King and A. F. G. Wyatt, Proc. Roy. Soc. Lond. A, **322**, 355 (1971).
 - [2] P. Roche, G. Delville, N.J Appleyard and F.I.B. Williams, J. Low Temp. Phys. **106**, 565 (1997).
 - [3] K. R. Atkins, Can. J. Phys. **31**, 1165 (1953).
 - [4] H. J. Lauter, H. Godfrin, V. L. P. Frank and P. Leiderer, Phys. Rev. Lett. **68**, 2484 (1992).
 - [5] H. J. Lauter, H. Godfrin and P. Leiderer, J. Low Temp. Phys. **87**, N 3-4, 425 (1992).
 - [6] C. C. Grimes and G. Adams, Phys. Rev. Lett. **36**, 145 (1976).
 - [7] D. Coimbra, S. S. Sokolov, J.-P. Rino and Nelson Studart, Phys. Rev. B **74**, 035411 (2006).
 - [8] M. Brown and A. F. G. Wyatt, J. Phys. Condens. Mat **15**, 4717 (2003).
 - [9] V. U. Nayak, D. O. Edwards and N. Masuhara, Phys. Rev. Lett. **50**, 990 (1983).
 - [10] A. F. G. Wyatt, M. A. H. Tucker and R. F. Cregan, Phys. Rev. Lett. **74**, 5236 (1995).
 - [11] G. E. Volovik, J. Low Temp. Phys. **145**, 337 (2006).
 - [12] P. Roche, G. Delville, K.O. Keshishev, N.J Appleyard and F.I.B. Williams, Phys. Rev. Lett. **75**, 3316 (1995).
 - [13] L. Pitaevskii and S. Stringari, Phys. Rev. B **45**, 13133 (1992).
 - [14] I. N. Adamenko, K. E. Nemchenko and I. V. Tanatarov, Phys. Rev. B **67**, 104513 (2003).
 - [15] I. N. Adamenko, K. E. Nemchenko and I. V. Tanatarov, Phys. Rev. B **77**, 174510 (2008).
 - [16] K. R. Atkins, Phys. Rev. **116**, 1339 (1959).
 - [17] A. Lastri, F. Dalfovo, L. Pitaevskii and S. Stringari, J. Low Temp. Phys. **98**, Nos. 3/4, 227 (1995).
 - [18] V. D. Natsik, Low Temp. Phys. **33**, 999 (2007) [Fiz. Nizk. Temp. **33**, 1319, (2007)].
 - [19] I. N. Adamenko, K. E. Nemchenko and I. V. Tanatarov, J. Phys.: Conf. Series **150**, No.3, 032107 (2009).
 - [20] L. Pitaevskii, Zh. Eksp. Teor. Fiz. **36**, 1168 (1959) [Sov. Phys. JETP **9**, 830 (1959)].
 - [21] L. D. Landau, E. M. Lifshitz, *Fluid Mechanics (Course of Theoretical Physics, Vol. 6)*, Pergamon Press, London (1987).
 - [22] I. N. Adamenko, K. E. Nemchenko, I. V. Tanatarov and A. F. G. Wyatt, J. Phys.: Cond. Mat. **20**, 245103 (2008).
 - [23] R. J. Donnelly, J. A. Donnelly and R. N. Hills, J. Low Temp. Phys. **44**, 471 (1981).